

# Spatial organization of active and inactive genes and noncoding DNA within chromosome territories

Nicola L. Mahy, Paul E. Perry, Susan Gilchrist, Richard A. Baldock, and Wendy A. Bickmore

Medical Research Council Human Genetics Unit, Edinburgh EH4 2XU, United Kingdom

The position of genes within the nucleus has been correlated with their transcriptional activity. The inter-chromosome domain model of nuclear organization suggests that genes preferentially locate at the surface of chromosome territories. Conversely, high resolution analysis of chromatin fibers suggests that chromosome territories do not present accessibility barriers to transcription machinery.

To clarify the relationship between the organization of chromosome territories and gene expression, we have used fluorescence in situ hybridization to analyze the spatial organization of a contiguous ~1 Mb stretch of the Wilms' tumor, aniridia, genitourinary anomalies, mental retardation syndrome region of the human genome and the syntenic region in the mouse. These regions contain constitutively expressed genes, genes with tissue-restricted patterns of

expression, and substantial regions of intergenic DNA. We find that there is a spatial organization within territories that is conserved between mouse and humans: certain sequences do preferentially locate at the periphery of the chromosome territories in both species. However, we do not detect genes necessarily at the periphery of chromosome territories or at the surface of subchromosomal domains. Intraterritory organization is not different among cell types that express different combinations of the genes under study.

Our data demonstrate that transcription of both ubiquitous and tissue-restricted genes is not confined to the periphery of chromosome territories, suggesting that the basal transcription machinery and transcription factors can readily gain access to the chromosome interior.

## Introduction

There is a well-established functional link between chromatin structure at the level of the nucleosome and gene expression (Jenuwein and Allis, 2001). However, the functional significance of higher-order chromatin structures in transcription remains unclear and has been examined at different levels; from large scale structures above the 30-nm fiber to whole chromosome territories (Mahy et al., 2000). It was thought that large scale chromatin organization above the 30-nm fiber might affect transcription by presenting an accessibility barrier to large protein complexes (Zirbel et al., 1993; Kurz et al., 1996). Hence, it has been proposed that

transcription and RNA processing might occur in a space between territories called the interchromosome domain (ICD)\* compartment (for review see Cremer and Cremer, 2001). In support of this model, specific gene transcripts and components of the splicing machinery have been reported to concentrate at the border of chromosome territories (Zirbel et al., 1993). However, poly(A) RNA is not excluded from chromatin domains, and nascent RNA can be seen deep within chromosome territories (Abranches et al., 1998; Verschure et al., 1999). The idea of a compact chromosome territory that would act as a barrier to the transcription machinery is contradicted by studies of chromatin fibers at higher resolution by both light microscopy and EM (Belmont et al., 1999).

If transcription does occur close to the surface of chromosome territories, genes should preferentially be found there, and noncoding sequences should be more internal. The intraterritory positions of a small number of individual genes from scattered genomic locations have been examined. In one report, three coding regions of the human genome were all located in the periphery of their respective chromosome territories independent of transcriptional status, whereas a noncoding sequence was not (Kurz et al., 1996). An active gene has also been found in a more peripheral location

Address correspondence to Wendy A. Bickmore, MRC Human Genetics Unit, Crewe Rd., Edinburgh, EH4 2XU, UK. Tel.:44-131-332-2471. Fax: 44-131-343-2620. E-mail: W.Bickmore@hgu.mrc.ac.uk

\*Abbreviations used in this paper: 2D, two-dimensional; 3D, three-dimensional; BAC, bacterial artificial chromosome; ES, embryonic stem; FISH, fluorescence in situ hybridization; ICD, interchromosomal domain/interchromatin domain; MAA, methanol acetic acid (3:1 vol/vol); Mb, megabase; MHC, major histocompatibility complex; pFa, paraformaldehyde; RT, reverse transcriptase; WAGR, Wilms' tumor, aniridia, genitourinary anomalies, mental retardation; Xa, active X chromosome; Xi, inactive X chromosome.

Key words: chromatin; chromosome territories; nuclear organization; synteny; transcription

within the active X chromosome (Xa) territory than its inactive counterpart in the inactive X chromosome (Xi) territory (Dietzel et al., 1999). The imprinted SNRPN genes are found at the periphery of both chromosome 15 homologues (Nogami et al., 2000). Over larger regions, it has been shown that the gene-rich major histocompatibility complex (MHC) lies on large chromatin loops that extend away from the surface of the bulk chromosome 6 territory that is detectable with a chromosome paint (Volpi et al., 2000). An extreme interpretation of these data is that most (active) genes lie on the surface of chromosome territories. However, with the exception of the Xi, both early and late replicating DNA that are usually equated with gene-rich and gene-poor domains, respectively, appear to be distributed throughout chromosome territories (Visser et al., 1998). Similarly, the most GC-rich fraction of the human genome (which has a high gene density) is also distributed throughout the volume of territories (Tajbakhsh et al., 2000).

Models of higher-order chromatin fiber and chromosome organization have implications for the spatial organization of genomic DNA in the nucleus both at the long range (chromosome band) level and at a more local megabase (Mb) level. To investigate the relationships between the organization of chromosome territories and gene expression, we have used fluorescence in situ hybridization (FISH) on both two-dimensional (2D) and three-dimensional (3D) samples to analyze the spatial organization of a contiguous 1 Mb stretch of the human genome and the syntenic region in the mouse. We have used cell types that express different repertoires of the genes from this region.

Distal human chromosome 11p13 is well mapped and sequenced because of its involvement in the Wilms' tumor, aniridia, genitourinary anomalies, mental retardation (WAGR) syndrome. It is moderately gene rich (Craig and Bickmore, 1994; Fantes et al., 1995; Gawin et al., 1999) and contains both ubiquitously expressed genes and genes whose expression is tissue restricted (Kent et al., 1997; Gawin et al., 1999; Kleinjan et al., 2002). There are also large (~300 kb) intergenic stretches of DNA (Kent et al., 1997; Gawin et al., 1999). Gene order and spacing are conserved at the region of conserved synteny on mouse chromosome 2 (MMU2E) (P. Gautier, personal communication) ([http://www.ensembl.org/Mus\\_musculus/](http://www.ensembl.org/Mus_musculus/); <http://www.ncbi.nlm.nih.gov/Omim/Homology/human11.html>). We have compared the organization of these genomic regions to a more distal region on human chromosome 11 (HSA11) (11p15) and its region of conserved synteny in the mouse MMU7.

Our data show that there is spatial organization within chromosome territories. However, genes from 11p13 or MMU2E do not preferentially localize at the periphery of their chromosome territories. All of the 11p13 loci studied, including expressed genes, have a mean position well within the bulk chromosome territory compared with a locus from 11p15 that locates at the territory edge. Tissue-restricted genes are not relocated to the territory periphery in expressing cells.

We conclude that in general there is no gross remodeling of chromosome territory organization to accommodate small changes in gene expression within mammalian

cells. Rather, it is more likely that small local changes in large scale chromatin fiber conformation accompany gene expression (Belmont et al., 1999). Our data may be compatible with the modified ICD model that suggests that this compartment penetrates into territories, ending at the surface of compact chromosomal subdomains of 0.3–0.45  $\mu\text{m}$  diameter (Verschure et al., 1999; for review see Cremer and Cremer, 2001). Chromatin fibers containing transcriptionally active DNA may be then be decondensed at the surface of these sub-domains or extend into the interchromatin spaces (Verschure et al., 1999). However, although we have found that a ubiquitously expressed gene is indeed located at the surface of, or outside of, such subdomains and although adjacent noncoding DNA is located within the compact subdomain, we find no clear correlation between chromosome territory subdomains and the expression of tissue-restricted genes.

## Results

### Active genes from 11p13 do not locate preferentially at the chromosome territory surface

It has been suggested that genes are preferentially located in the periphery of chromosome territories (Kurz et al., 1996; Dietzel et al., 1999; Volpi et al., 2000; Cremer and Cremer, 2001). However, the positions of only a small number of individual genes, usually from scattered chromosomal locations, have been examined. To determine if genes from a contiguous region of the human genome are located together at the chromosome periphery, we examined the intrachromosomal organization of a megabase stretch of the human genome.

Within the distal ~1 Mb of human 11p13, there are four known genes. *RCN* (Kent et al., 1997) and *PAXNEB* (Kleinjan et al., 2002) are ubiquitously expressed, whereas the expression of *WT1* and *PAX6* is tissue restricted (Hastie, 1994; Xu et al., 1999). Gene order is conserved at the syntenic region on MMU2E, and there are large intergenic regions (~300 kb) between *WT1* and *RCN* and between *RCN* and *PAX6* in both man and mouse (Kent et al., 1997; Gawin et al., 1999; P. Gautier, personal communication). This is confirmed by the compression of these genes in the region of conserved synteny from *Fugu rubripes* (Miles et al., 1998).

*WT1* and *PAX6* are separated by 700 kb of genomic DNA. FISH to 2D preparations showed that within human lymphoblast nuclei the mean-square interphase distance ( $r^2$ ) ( $0.87 \pm 0.11 \mu\text{m}$ ) between signals from two cosmids encompassing *WT1* and *PAX6* (Fantes, 1997) is intermediate to the values reported for gene-poor (G-band) and very gene-rich (T-band) regions of the human genome (Yokota et al., 1997), consistent with the moderate gene density of this R-band region of the human genome (Fantes et al., 1995). Therefore, there is sufficient spatial resolution at interphase between the loci under study to detect any significant differences in their intraterritory distribution.

Using reverse transcriptase (RT)-PCR, we confirmed the expression of *RCN* and *PAXNEB* in lymphoblastoid cells and primary fibroblasts. *WT1* and *PAX6* are not expressed (Fig. 1). Cosmids encompassing the human WAGR region were first hybridized together with a paint for 11p to MAA-

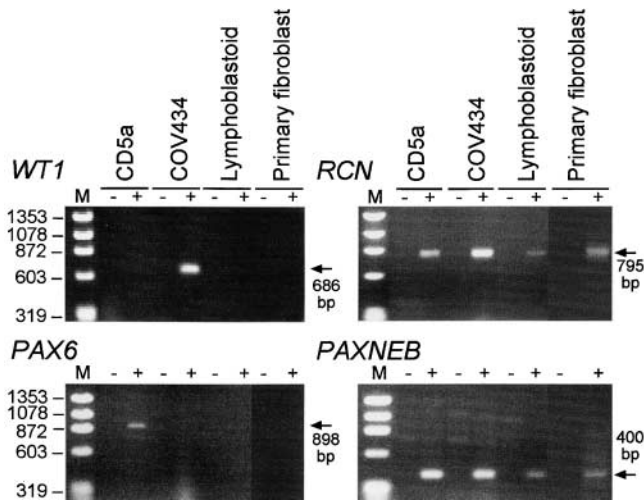


**Figure 1. Expression of WAGR locus genes in human cell lines.** Transcripts from WAGR locus genes were amplified by RT-PCR. Amplification was specific to the RNA and not from contaminating DNA, since there was no productive amplification from control –RT samples. The ovarian carcinoma cell line COV434 expresses the *WT1* gene; *RCN* is expressed in all four cell lines tested; *PAX6* is expressed only in the lens epithelium-derived cell line CD5a; *PAXNEB* is expressed in all four cell lines. M, size markers in base pairs.

fixed lymphoblast nuclei (Fig. 2 a). Images from 50 randomly selected nuclei were analyzed per locus. The distance ( $\mu\text{m}$ ) between the center of each locus signal to the nearest chromosome territory edge was calculated as described (see Materials and methods). For the expressed gene *RCN*, 60% of signals were  $\geq 0.4 \mu\text{m}$  from the territory edge (Fig. 3 b). Similar figures (61 and 65%) were seen for the linked inactive gene *PAX6* and the noncoding D11S324 locus. This was in contrast to a locus (D11S12) from a more distal chromosome band 11p15.4 for which the bulk of signals were at the territory edge and only 27% of signals were  $\geq 0.4 \mu\text{m}$  from the territory edge (Fig. 2 b and Fig. 3 b). The mean distances of all the WAGR probes from the territory edge (0.45–0.65  $\mu\text{m}$ ) were significantly greater than that for D11S12 (Fig. 3 c) and other loci from 11p15 (unpublished data). WAGR probes were not found preferentially at the territory edge but neither were they in the center of the territory. The average distance between the territory centroid and edge was 1.15  $\mu\text{m}$ . Because we found that territories detected in G2 cells were larger than those in G1 cells (unpublished data), we also normalized actual distances relative to the radius of a circle of equal area to the chromosome territory. Values of 0 and 1 then equate to theoretical positions at the territory edge or center, respectively (Fig. 3 c). Because territories are not circular, the actual position of the

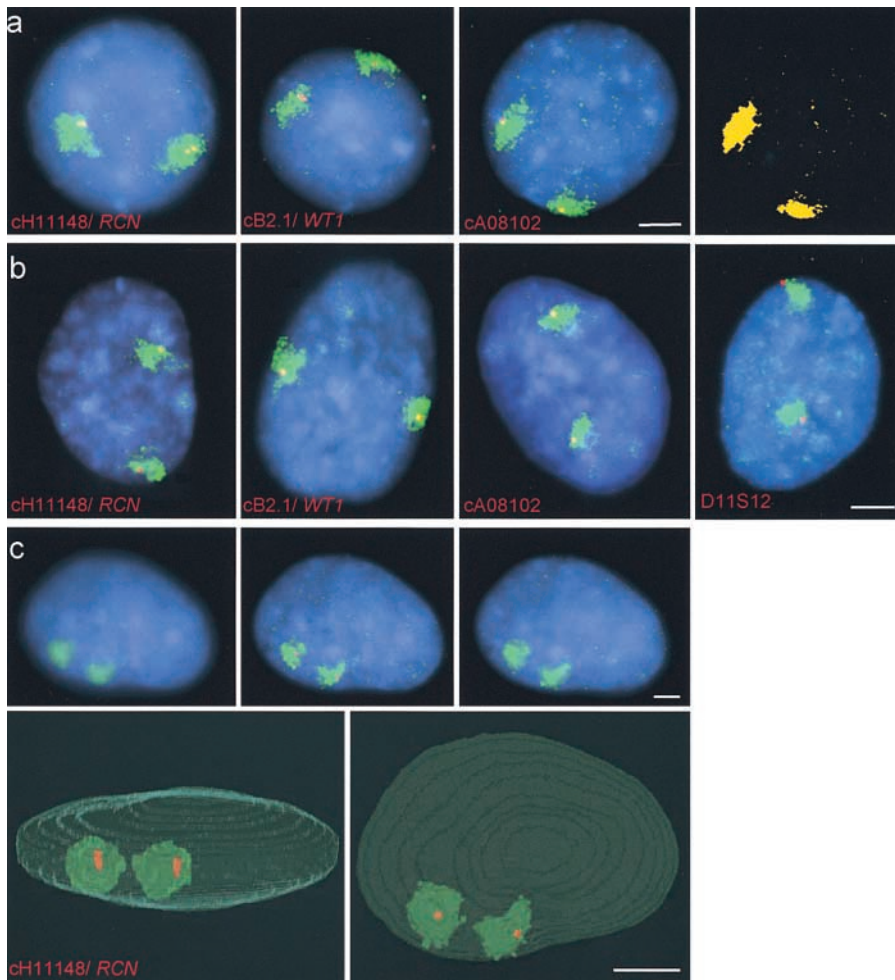


**Figure 2. Visualizing intraterritory position of loci from human 11p13 and 11p15.** FISH of selected cosmids (red) from the WAGR region (11p13) or 11p15 together with an 11p paint (green) to MAA-fixed FATO lymphoblast (a) and 1HD primary fibroblast (b) nuclei. cH11148 detects the ubiquitously expressed *RCN* gene. cB2.1 contains the *WT1* gene that is not expressed in either of the two cell types. cA08102 is from the intergenic region between *RCN* and *PAX6* (D11S323) (Fig. 3 a). D11S12 is an anonymous marker from 11p15.4. The last image in panel a shows the territory segmentation masks for the cA08102 image. (c) Three plane images through a 3D preserved pFa-fixed fibroblast nucleus at 1- $\mu\text{m}$  intervals in the z direction after hybridization with probes to *RCN* and 11p. Views of an MAPaint reconstruction of the same nucleus after delineation of the nucleus, chromosome territory, and locus probe domain are shown at 0 and 90° rotation about the x axis. Nuclei were counterstained with DAPI (blue). Bars, 5  $\mu\text{m}$ .



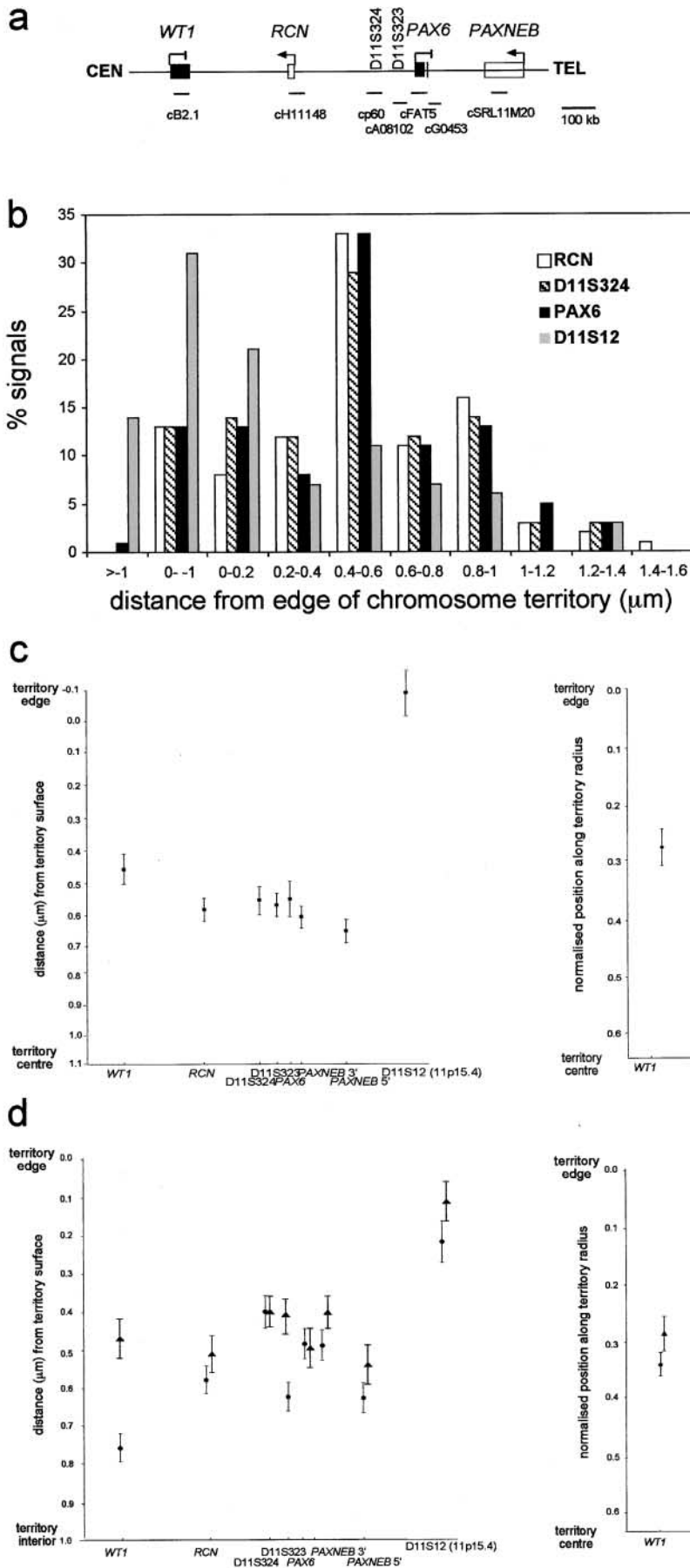


**Figure 3. Intraterritory organization of the human WAGR region.** (a) Position of genes within the distal 1 Mb of human 11p13 DNA relative to cosmids used in this study. Open boxes represent ubiquitously expressed genes. Filled boxes represent genes with tissue-restricted expression. Arrows indicate the direction of transcription. The bar represents 100 kb. (b) Histogram showing the distribution of signals relative to the territory edge (in  $\mu\text{m}$ ) for expressed (*RCN*) and nonexpressed (*PAX6*) genes from 11p13, a noncoding region of 11p13 (*D11S324*), and a marker (*D11S12*) from 11p15 in MAA-fixed FATO lymphoblast nuclei. (c) Mean position ( $\pm$  SEM) of 11p13 and 11p15 probes within the 11p territory of MAA-fixed lymphoblast nuclei. Distance in  $\mu\text{m}$  is shown on the left, and distances normalized for territory size are shown on the right where values of 0 and 1 equate to positions at the territory edge or the theoretical territory center, respectively ( $n \approx 100$ ). The average distance between territory centroid and nearest territory edge in these cells was 1.14  $\mu\text{m}$ , and the normalized position of the measured territory center is 0.64. Intercepts for the graphs are thus placed at these values. (d) Mean position of 11p13 and 11p15 probes within the 11p territory of MAA-fixed fibroblast nuclei (●) or in fibroblast nuclei fixed in pFa to preserve 3D structure (▲).

territory centroid in lymphoblasts was at  $0.65 \pm 0.02$  (Fig. 3 c). Using analysis of variance, there was no significant difference between the positions of any of the WAGR loci examined ( $p = 0.68$ ), but WAGR probes were located further inside of the chromosome territory than D11S12 ( $p < 0.01$ ) (Fig. 3 c).

Territory organization may vary through the cell cycle, for example, before, during, or after replication. Cosmid signals often appear as single spots of hybridization before replication of the locus that they detect and as paired dots (Fig. 2 a) after replication (Bickmore and Carothers, 1995). We detected no significant difference ( $p = 0.41$ ) between the intraterritory position of a locus before and after its replication. Similarly, the variance in locus position within the two territories of homologous chromosomes within a cell was not less than that between cells in an unsynchronized population, indicating that territory organization within homologous chromosome territories of nuclei is independent.

Human primary fibroblasts were also subjected to the same analysis (Fig. 2 b). All of the 11p13 probes tested were located inside of the chromosome territories compared with D11S12 (Fig. 3 d).

Analysis of 2D specimens allows for statistical analysis of large numbers of images. However, it was important to establish that data from these preparations was consistent with intraterritory organization in cells in which 3D nuclear architecture had been preserved (Kurz et al., 1996; Croft et al., 1999; Volpi et al., 2000). Using human HT1080 cells that stably express centromere-localized GFP-tagged CENP-A, we first determined that the spatial organization of centromere sequences was not perturbed during neither the fixation procedure with 4% paraformaldehyde (pFa) nor the subsequent FISH procedures. We took image stacks of centromere-localized GFP signal in the living cells (Fig. 4 a) and then in the same cells after pFa fixation (Fig. 4 b). Lastly, hybridization signal from an  $\alpha$ -satellite probe was analyzed in these same cells after 3D FISH (Fig. 4 c). The images from the three stages of the experiment were comparable. Signals from the detection of  $\alpha$  satellite by FISH were generally larger and more variable than those from GFP-CENPA (Fig. 4). This is because similar amounts of CENPA are assembled into the kinetochore of every chromosome, whereas the size of  $\alpha$ -satellite arrays varies amongst centromeres and extends beyond the kinetochore itself. In addition, the efficiency with which the  $\alpha$ -satellite probe detects each centromere will vary depending on the exact sequence of the arrays. We measured the distance separating pairs of centromeres ( $n = 10$ ). The distance between two centromeres in living cells decreased by an average of  $0.1 \mu\text{m}$  upon fixation with pFa. After 3D FISH, the distance between pairs of centromeres had increased by  $0.18 \mu\text{m}$  compared with living cells. Hence, any nuclear reorganization brought about by the 3D FISH process is small and does not affect our conclusions.

We then analyzed the intraterritory position of loci from the WAGR region in 3D preserved primary fibroblast nuclei (Fig. 2 c). Measurements were made on 15–18 randomly selected nuclei per locus. Probes from the human WAGR locus (Fig. 3 a) were on average positioned  $0.4$ – $0.5 \mu\text{m}$  away

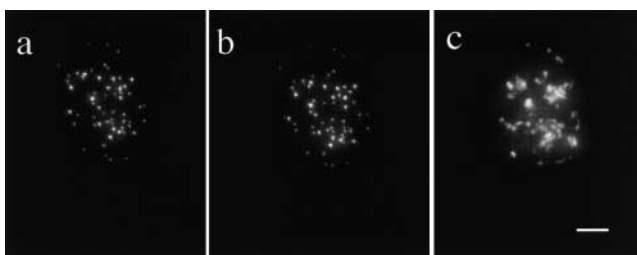


Figure 4. **3D FISH does not perturb nuclear organization.** Human HT1080 fibrosarcoma cells stably expressing a CENPA–GFP fusion protein. GFP fluorescence in living cells (a), GFP fluorescence in the same cell after fixation in 4% pFa (b), and hybridization signal from an  $\alpha$ -satellite probe in the same cell after 3D FISH (c). Single image planes are shown without deconvolution. Note that this cell line is aneuploid. Bar,  $5 \mu\text{m}$ .

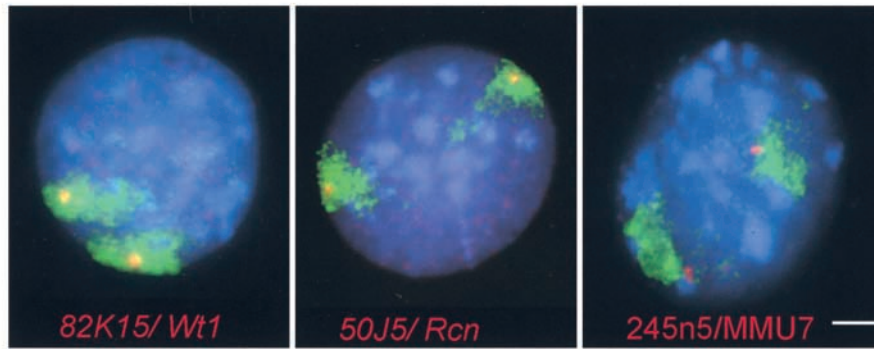
from the edge of the chromosome territory. These distances were generally a bit smaller than those measured in 2D samples, but the normalized position within the territory was similar between 2D and 3D specimens (Fig. 3 d). This suggests a general swelling of the chromosome territory in 2D preparations but no reorganization of sequences with respect to each other (Volpi et al., 2000). In 3D preparations, the 11p15.4 locus D11S12 was located at the territory periphery as in 2D preparations.

Therefore, we conclude that there is no preference for genes from 11p13 to locate at the periphery of the 11p territory, as defined in FISH by a chromosome paint, compared with intergenic sequences from the same region. Ubiquitously expressed genes can be transcribed at a mean distance of  $0.6 \mu\text{m}$  away from the visible territory edge. However, there is a reproducible spatial compartmentalization within the chromosome 11 territory: a locus D11S12 from 11p15.4 and other 11p15 loci (unpublished data) are located preferentially at the territory edge.

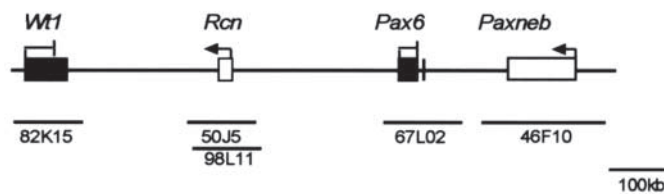
### Evolutionary conservation of chromosome architecture

Gene order and spacing are conserved at the murine WAGR region of synteny on MMU2E (P. Gautier, personal communication; [http://www.ensembl.org/Mus\\_musculus/](http://www.ensembl.org/Mus_musculus/); <http://www.ncbi.nlm.nih.gov/Omim/Homology/human11.html>) (Fig. 3 a and Fig. 5 b). To investigate whether this linear sequence conservation also extends to the spatial organization of the locus, we investigated the intraterritory position of genes spanning the murine WAGR locus. Bacterial artificial chromosomes (BACs) encompassing this region (Fig. 5 b) were hybridized together with a paint for MMU2 to MAA-fixed embryonic stem (ES) cell nuclei. Compared with the human WAGR locus on 11p (Fig. 3), genes and intergenic DNA from the mouse WAGR region are located even further ( $0.75$ – $1 \mu\text{m}$ ) away from the edge of the MMU2 territory (Fig. 5 c). This is due to the larger size of the MMU2 territory compared with HSA11p (200 versus 50 Mb) ([http://www.ensembl.org/Mus\\_musculus/](http://www.ensembl.org/Mus_musculus/) and [http://www.ensembl.org/Homo\\_sapiens/](http://www.ensembl.org/Homo_sapiens/)), and territory centroids were on average  $1.58 \mu\text{m}$  away from the nearest territory edge. Indeed the positions of the human and mouse WAGR loci, normalized to take account of territory size,

a



b



c

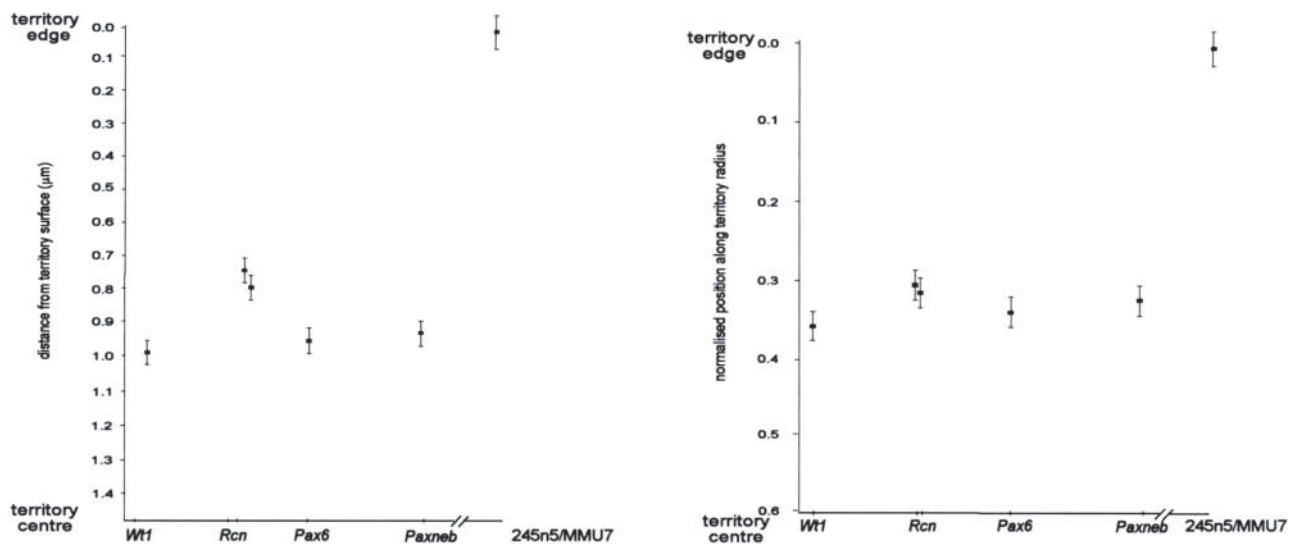


Figure 5. **Intraterritory organization in the mouse.** (a) FISH of BACs 82K15 (*Wt1*) and 50J5 (*Rcn*) (red) from the WAGR region together with a paint for MMU2 (green) or BAC 245n5 (red) with an MMU7 paint (green) to MAA-fixed ES cell nuclei. Nuclei were counterstained with DAPI (blue). Note the yellow color of the (red) probe signals located within the (green) MMU2 chromosome territories and the red color of the MMU7 probe signal at the territory edge. Bar, 5  $\mu\text{m}$ . (b) Map of the mouse region of conserved synteny to WAGR at human 11p13 on MMU2, relative to the BACs used as probes. (c) Mean position ( $\pm$  SEM) of MMU2 and seven probes within chromosome territories of MAA-fixed ES cell nuclei. Distance in  $\mu\text{m}$  is shown on the left, and distances normalized for territory size are shown on the right where values of 1 and 0 equate to positions at the theoretical territory center or periphery, respectively ( $n \approx 100$ ). The mean distance between the MMU2 territory centroid and nearest territory edge was 1.48  $\mu\text{m}$  in ES cells, and the normalized position of the territory centroid was 0.58. Graph intercepts are placed at these values.

are very similar (Fig. 5 c). On human 11p, sequences from 11p15 are at the territory periphery (Fig. 3). The murine region of conserved synteny to human 11p15 is on MMU7 (<http://www.ncbi.nlm.nih.gov/Omim/Homology/human11.html>). DNA hybridizing to a BAC 245N5 from this region (Engemann et al., 2000) was also found to locate

at the edge of the MMU7 territory (Fig. 5, a and c). Therefore, in addition to primary sequence conservation there is conservation of relative intraterritory organization between regions of the mouse and human genomes that are in conserved synteny, suggesting that this organization has functional significance.

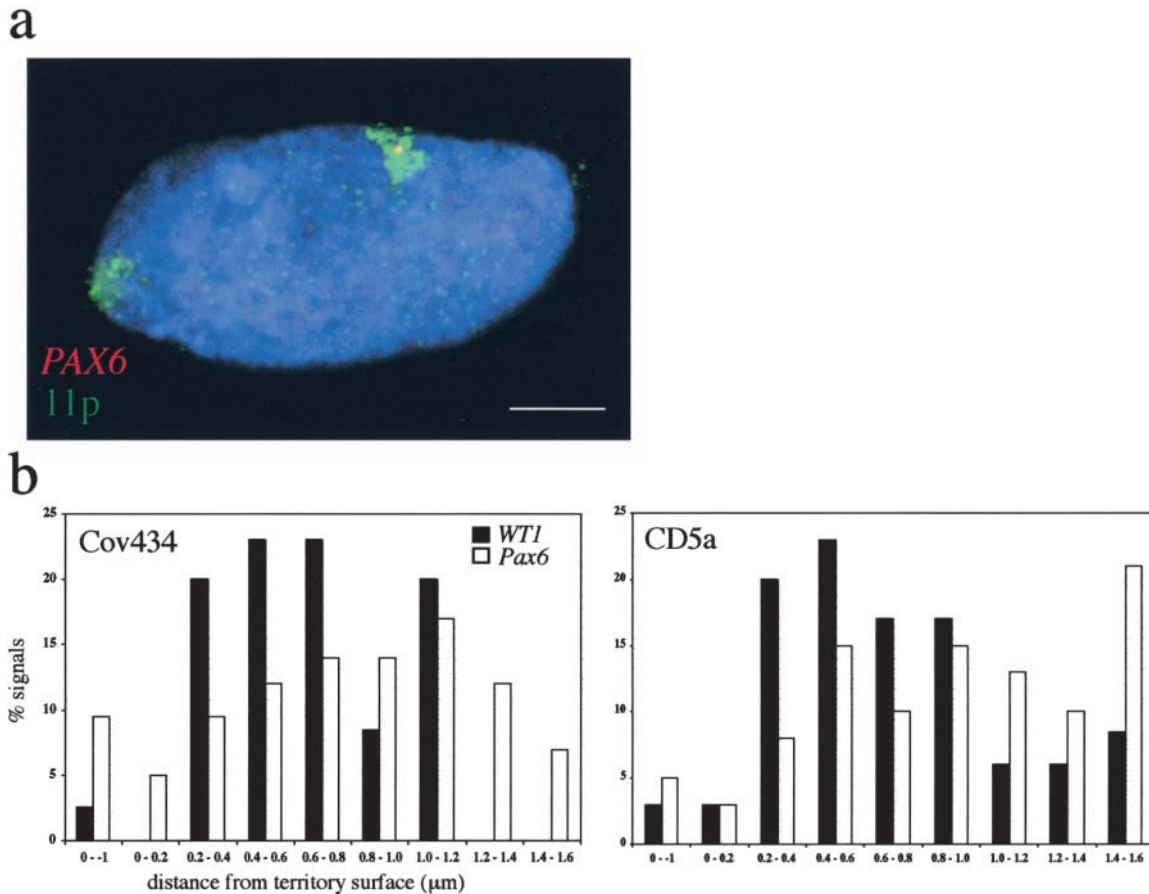


Figure 6. **Intraterritory position of a tissue-restricted gene.** (a) 3D FISH to detect *PAX6* (red) within the 11p territory (green) of pFa-fixed CD5a lens epithelial cells in which *PAX6* is expressed (Fig. 1). DNA is counterstained with DAPI (blue). Only a single deconvolved image plane is shown; hence, the probe signal can only be seen within one of the territories. Bar, 5  $\mu\text{m}$ . (b) Histogram showing the distribution of 3D FISH signals relative to the territory edge (in  $\mu\text{m}$ ) for *PAX6* and *WT1* in pFa-fixed COV434 cells (*WT1*-expressing) and CD5a cells (*PAX6*-expressing).

### Changes in gene expression do not require spatial reorganization of 11p13

Transcription of genes from the WAGR region from within the volume of the chromosome territory could be restricted to ubiquitously expressed genes that do not require specialized transcription factors for their expression. To examine whether expression of tissue-restricted genes could also take place away from the periphery of chromosome territories, the organization of the human WAGR locus was analyzed in nuclei from cell lines that in addition to *RCN* and *PAXNEB* also express tissue-restricted genes. RT-PCR analysis showed that CD5a, a lens epithelial cell line, expresses *PAX6* and that COV434, an ovarian carcinoma cell line, expresses *WT1* (Fig. 1). Immunofluorescence (*WT1*) and immunohistochemistry (*PAX6*) showed that all cells in the populations express the proteins (unpublished data).

The spatial organization of the *WT1* and *PAX6* genes was assessed in 3D-preserved CD5a and COV434 cells. *PAX6* is not preferentially located at the periphery of the 11p territory in CD5a cells (Fig. 6 a); 84% of FISH signals were  $\geq 0.4$   $\mu\text{m}$  away from the territory edge (Fig. 6 b). 75% of *WT1* signals were  $\geq 0.4$   $\mu\text{m}$  from the territory edge in COV434 cells (Fig. 6 b). Therefore, we find no evidence that tissue-specific genes are repositioned to the periphery of

chromosome territories to facilitate transcription, and transcription factors for such genes must be able to access their targets inside of chromosome territories.

### Genes and subchromosomal domains

The original ICD compartment model described chromosome territories as compact objects surrounded by a network of channels that connect to the nuclear pores (Zirbel et al., 1993; Kurz et al., 1996). However, the ICD compartment has been extended recently to include small channels penetrating chromosome territories, ending between 1-Mb domains of perhaps 0.3–0.45  $\mu\text{m}$  diameter (Verschure et al., 1999; Cremer and Cremer, 2001). Actively transcribed loci are thought to be positioned at the surface of these compact subchromosomal domains rather than at the surface of entire chromosomes, depositing newly synthesized RNA directly into the extended interchromatin space (Verschure et al., 1999). This is more compatible with high resolution observation of large scale chromatin fibers of different compaction (Belmont et al., 1999). In accordance with this idea, in 3D preserved fibroblast nuclei we found a preference for the ubiquitously transcribed *RCN* gene to be positioned in areas of the chromosome territory unlabeled by FISH (50% of cases,  $n = 14$ ). In a single image plane, the probe appears as a red signal, indicating no colo-



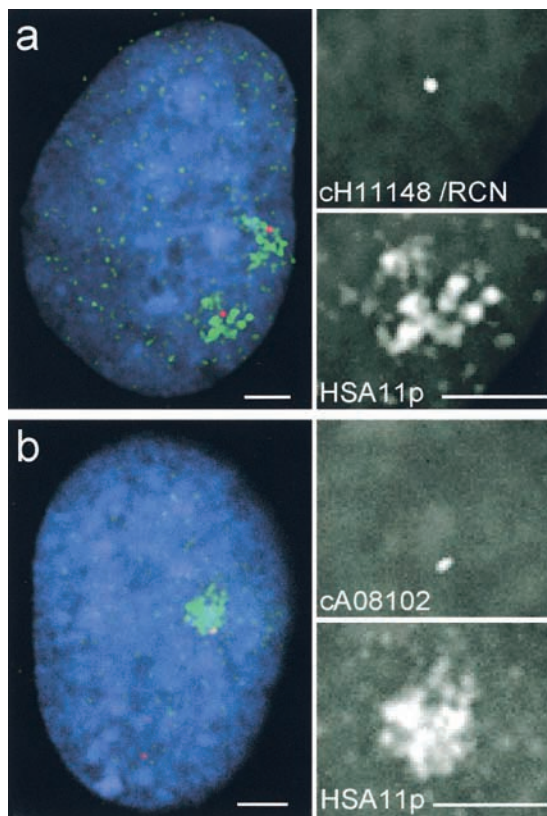


**Figure 7. Chromosome territory substructure.** FISH of the cH11148 cosmid probe (a), which detects the ubiquitously expressed RCN gene, and the cA08102 cosmid (b), which represents a nontranscribed intergenic sequence (D11S323) from WAGR (both red), together with a paint for HSA11p (green) to 3D preserved pFa-fixed primary fibroblast nuclei. Both chromosome territories are present in the same z axis plane in panel a but not in panel b. Magnified views of gray scale images of one probe signal from each nucleus are shown above the corresponding deconvolved chromosome territory signal. Bars, 2.5  $\mu$ m.

calization with the deconvolved green chromosome territory signal (Fig. 7 a). This contrasted strongly with a probe cA08102, detecting noncoding intergenic DNA  $\sim$ 300 kb distal of RCN (Fig. 3 a). No signals from this probe ( $n = 13$ ) were found outside of the compact territory subdomains detected by FISH with a chromosome paint. Instead, the probe signal was frequently (61.5%,  $n = 13$ ) positioned within a region of densely stained chromatin. Hence the probe signal appeared yellow due to its colocalization with the labeled chromosome subdomain (Fig. 7 b). Our data supports a correlation between the position of DNA relative to chromosome subdomains and gene expression (Verschuer et al., 1999), at least in the case of housekeeping genes. However, the position of genes with a tissue-restricted expression pattern with respect to subdomains was less clear. At this level of analysis, the position of the *WT1* and *PAX6* genes within chromosome subdomains from fibroblasts, COV434, and CD5a cells did not appear to be correlated with their expression pattern (unpublished data). Therefore, there is not a consistent correlation between transcription and chromosome territory substructure defined by chromosome paint. Furthermore, unlabeled areas of a chromosome territory cannot be “holes” devoid of chromatin, since we

find gene loci located in these regions. It is likely that unlabeled regions represent decondensed chromatin fibers within the territory that cannot be detected by FISH with chromosome paints rather than defined interchromatin channels.

## Discussion

### Transcription of genes can occur within the interior of a chromosome territory

Components of the splicing machinery and specific gene transcripts of an integrated human papilloma virus genome are often excluded from the interior of chromosome territories (Zirbel et al., 1993). Furthermore, three coding regions of the human genome have been observed at the periphery of chromosome territories, and a single nontranscribed sequence was randomly distributed or more internally positioned (Kurz et al., 1996). Within the context of the ICD compartment model of nuclear organization (Cremer and Cremer, 2001), an extreme interpretation of these data is that most or all genes lie on the periphery of chromosome territories and that the territory interior is filled with intergenic sequence (Zirbel et al., 1993; Kurz et al., 1996). However, here we have shown that both coding and noncoding sequences from 11p13 are similarly located inside of the HSA11p territory. Both ubiquitously expressed genes and genes with a tissue-restricted expression pattern can be transcribed from within the territory interior (Figs. 3 and 6). This argues against the concept of a compact chromosome territory and indicates that the basal transcription machinery and transcription factors must be able to readily access chromatin located within the interior of chromosome territories. Our data indicate that large scale chromatin remodelling to position genes on the surface of a territory is not required to facilitate transcription but rather that any changes to the chromatin fiber are likely to be local (Belmont et al., 1999).

Therefore, our data question the extent to which the organization of chromosomes within territories can contribute to control of gene expression. Replication has been shown to take place in foci located throughout the entire chromosome territory volume (Visser et al., 1998). This demonstrates that activity of macromolecular enzyme complexes takes place throughout chromosome territories and is not confined to the territory surface (Zirbel et al., 1993; Kurz et al., 1996). In addition, transcription sites have been visualized throughout the nucleus (Abranches et al., 1998; Verschuer et al., 1999), and using FRAP nuclear proteins with diverse functions and distinct distribution patterns have been shown to diffuse rapidly throughout the entire nucleus (Phair and Misteli, 2000). The fact that the human WAGR locus is positioned inside the HSA11p chromosome territory rather than at its periphery is consistent with these observations.

### Intraterritory organization is not random and is conserved

Although we did not find genes from 11p13 preferentially at the periphery of the HSA11 territory, we did find that territories are spatially organized. In contrast to 11p13 DNA, sequences from 11p15 were preferentially located at the surface of the HSA11 territory (Fig. 3).



We extended our study of the WAGR locus to the syntenic region in the mouse. This is the first time that the organization of murine chromosome territories has been considered. We found that sequences, including expressed genes, from the murine WAGR locus were located in a similar relative position inside of the territory of MMU2 as the human region is within the HSA11p territory (Fig. 5). Likewise, the region of MMU7 in conserved synteny with HSA11p15 is located at the periphery of the MMU7 territory (Fig. 5). Conservation of sequence organization within chromosome territories suggests that it has functional significance, but it remains to be determined what that is. The conservation of spatial organization within chromosome territories is interesting in light of the conservation of territory position within the nucleus that has been seen in vertebrates (Croft et al., 1999; Boyle et al., 2001; Habermann et al., 2001; Tanabe et al., 2002).

### Small scale changes in the transcription profile of a region do not require territory reorganization

Three studies have indicated a role for active transcription in organizing gene position within a chromosome territory (Dietzel et al., 1999; Volpi et al., 2000; Williams et al., 2002). Volpi et al. (2000) noted a difference in the incidence of extrusion of chromatin containing the MHC locus from the surface of HSA6 in cell lines with different expression profiles of MHC genes. Inducing transcription from this region using IFN $\gamma$  increased the incidence of chromatin looping (Volpi et al., 2000). A relationship between transcription status and position was observed for a single gene within the Xa and Xi territories. The *SLC25A5* (previously *ANT2*) gene was more peripheral within the Xa chromosome from which it is actively transcribed than within the Xi territory in which it is silent (Dietzel et al., 1999).

Using cell lines that express the tissue-restricted *WT1* or *PAX6* genes (Fig. 1), we found no significant alteration of the intraterritory position adopted by the WAGR locus that correlated with increased gene expression. Genes that are inactive in lymphoblasts and fibroblasts were not relocated to the HSA11p territory surface when actively transcribed but rather remain within the chromosome territory in a position similar to those of neighboring ubiquitously active genes and noncoding sequences (Fig. 6).

Differences in intraterritory organization dependent on transcription status of associated genes were ascertained previously within the context of chromosome domains subject to large scale transcriptional differences. The MHC locus consists of families of genes with the same or a related function; therefore, all of the genes are subject to the same regulation kinetics (Volpi et al., 2000). Similarly, the human epidermal differentiation complex at 1q21 contains functionally related genes involved in keratinocyte differentiation. This region appears to be extended outside of the HSA1 territory in keratinocytes where the genes are highly expressed but not in lymphoblasts where they are silent (Williams et al., 2002). Transcriptional activation of a 90-Mb heterochromatic region containing 256 copies of the lac operator sequence has also been associated with large scale chromatin decondensation (Tumbar et al., 1999). Lastly, the Xi adopts a unique structure which differs from the Xa territory (Eils et al., 1996; Dietzel et al., 1999) and is generally devoid of sites of transcription (Ver-

schure et al., 1999). It is unclear how widely applicable observations made from study of X chromosome territory organization will be to the rest of the human karyotype.

### Do levels of chromatin packaging within territories contribute to control of gene expression?

A high resolution chromosome painting study has suggested that locally compacted and unfolded regions within chromosome territories form distinct subdomains of 0.3–0.45  $\mu$ m diameter and that chromatin is organized in such a way that transcriptionally active loci are at the surface of large scale chromatin fibers (Verschure et al., 1999). These data imply that limitations on protein accessibility within chromosome territories are likely to map to the periphery of large scale chromatin fibers or larger chromosome subdomains formed by the folding of these fibers. Transmission EM localization of uridine or BrUTP incorporation has shown heavy labeling at the edge of condensed large scale chromatin domains rather than at the surface of chromosomes itself (Fakan and Nobis, 1978; Wansink et al., 1996; Cmarko et al., 1999). Transcripts of 1 $\alpha$ 1 collagen located within the chromosome 17 territory similarly often coincide within holes in the chromosome paint (Clemson and Lawrence, 1996). Such observations have been used to extend the concept of the ICD (now interchromatin domain) to include channels penetrating into chromosome territories (Cremer and Cremer, 2001), ending in branches between 1 Mb and 100 kb chromatin loop domains. Transcription apparently occurring within chromosome territories is therefore actually occurring on the “surface” of chromosome subdomains (Verschure et al., 1999). In accordance with this idea, we found that a ubiquitously transcribed gene often colocalized with unlabeled or less intensely labeled areas of the chromosome territory, whereas the linked intergenic locus was positioned frequently in intensely labeled (compact) subdomains of the territory (Fig. 7). The fact that we found gene sequences themselves and not just their transcripts in apparent “holes” in the chromosome territory implies that these are not in fact channels devoid of chromatin but rather that they correspond to areas of decondensed chromatin fibers not detectable by chromosome painting. The positions of genes with a tissue-restricted expression pattern with respect to chromosome subdomains did not appear to correlate with their expression status. Therefore, the role of subchromosomal packaging in facilitating transcription remains open to debate and further investigation.

## Materials and methods

### Cell culture

Human FATO lymphoblasts (46XY) were grown in RPMI plus 10% FCS. Human 46XY primary fibroblasts (less than passage 12) and the human lens epithelium-derived cell line CD5A (a gift from A. Prescott, University of Dundee, Dundee, UK) were grown in DME plus 10% FCS. COV434 human ovarian (granulosa) carcinoma cells (Berg-Bakker et al., 1993) were grown in a 1:1 mixture of F10 and DME supplemented with 10% FCS. The murine ES cell line E14 (Hooper et al., 1987) was maintained on a gelatinized (0.1% in PBS) surface in MEM/BHK21 medium supplemented with 0.23% sodium bicarbonate, 1 $\times$  MEM nonessential amino acids, 2 mM glutamine, 1 mM sodium pyruvate, 50  $\mu$ M  $\beta$ -mercaptoethanol (all Life Technologies), 10% FCS (Sigma-Aldrich), and 100 U/ml soluble DIA/LIF (Sigma-Aldrich).

### Immunofluorescence and immunohistochemistry

WT1 protein was detected in COV434 cells by immunofluorescence using the C19 polyclonal antibody (Santa Cruz Biotechnology) that detects the COOH-terminal 19 amino acids of the protein and an FITC-conjugated

anti-rabbit secondary antibody (Jackson ImmunoResearch Laboratories). PAX6 protein was detected in CD5A cells (A. Seawright, personal communication) using AD1.5.6 and AD2.3.7 antibodies (1:1) raised against the NH<sub>2</sub>-terminal 206 amino acids of PAX6 (Engelkamp et al., 1999). Staining was visualized using Vectastain ABC Systems and NBT/BCIP substrate kits (Vector Laboratories).

### FISH

A paint for human chromosome 11p (HSA11p) was labeled with biotin-16-dUTP by PCR amplification (Guan et al., 1996; Croft et al., 1999). Cosmids from 11p (Fantes et al., 1995) were labeled by nick translation with digoxigenin-11-dUTP. This labeling scheme was adopted because the 11p chromosome territories detectable with biotin-labeled paint were brighter and more reproducible than those seen using digoxigenin-labeled paints. 210 ng paint and 50 ng cosmids were used per slide in a volume of 12  $\mu$ l together with 6  $\mu$ g human CotI DNA (GIBCO BRL) as competitor.

MMU2 paint (Jentsch et al., 2001) was amplified and biotin labeled by PCR using the degenerate primer 5'-CCGACTCGAG(N)<sub>6</sub>TACACC-3'. Mouse BACs, 82K15, 98L11, 67L02, and 46F10 were selected from a 129 library (Genome Systems, Inc.) (D.A. Kleinjan, personal communication) and labeled with digoxigenin by nick translation. 200 ng paint were used together with 100 ng BAC DNA per slide in a volume of 12  $\mu$ l with 14  $\mu$ g mouse CotI DNA (GIBCO BRL) added as competitor.

For 2D analysis, cells were swollen in 0.5% trisodium citrate/0.25% KCl before fixation in methanol acetic acid (MAA; 3:1 vol/vol) using standard procedures. Slide hybridization was as described previously (Fantes et al., 1995; Croft et al., 1999). To preserve 3D nuclear structure, human primary fibroblasts were grown on slides and fixed with 4% pFa/PBS for 10 min before FISH as described previously (Kurz et al., 1996; Croft et al., 1999).

To check the preservation of nuclear structure after 3D FISH on pFa-fixed cells, we analyzed the position of human centromeres in living and pFa-fixed cells and in the same cells after 3D FISH. Image stacks were taken of the GFP signal in living human HT1080 cells stably expressing a CENPA-GFP fusion protein that correctly localizes to centromeres (unpublished data). The GFP signals in the same nuclei were then imaged after fixation in 4% pFa/PBS for 10 min. The 3D FISH procedure was then performed on these slides using a biotinylated probe that detects  $\alpha$ -satellite sequences and that was generated by PCR amplification (Weier et al., 1991). After signal detection, the same cells were relocated on the slide, and image stacks were taken of the centromeric hybridization signals (Fig. 4).

Biotinylated probes were detected using fluorochrome-conjugated avidin (FITC or Texas red) (Vector Laboratories) followed by biotinylated antiavidin (Vector Laboratories) and a final layer of fluorochrome-conjugated avidin. Digoxigenin-labeled probes were detected with sequential layers of FITC-conjugated antidigoxigenin (BCL) and FITC-conjugated anti-sheep (Vector Laboratories). Slides were counterstained with 1  $\mu$ g/ml DAPI. 2D slides were examined using a ZEISS Axioplan fluorescence microscope equipped with a triple band-pass filter (Chroma #83000). Gray scale images were collected with a cooled CCD camera (Princeton Instruments Pentamax) and analyzed using custom IPLab scripts. For 3D analysis, a focus motor was used to collect images at 0.5- $\mu$ m intervals in the z direction from a ZEISS Axioplan using a Xillig CCD camera. 3D image stacks were analyzed using IPLab extensions and deconvolved using Hazebuster (Vaytek, Inc.). For random selection of nuclei for analysis, slides were scanned in a methodical manner, beginning at the top left hand corner, scanning to the right, then moving downwards and scanning the next row of nuclei from right to left, etc. Images of consecutive nuclei that had two chromosome territories in which locus signals were visible and that were not touching adjacent nuclei, since this interferes with segmentation (see below), were collected.

### Image analysis

The following script was used to analyze the position of loci within chromosome territories in 2D. Nuclear area was calculated from the segmented DAPI image. Background was removed from FITC and Texas red images as described previously (Croft et al., 1999). Locus-specific hybridization signals were automatically segmented, and a region of interest was manually defined around one of the signals (each locus signal was treated independently; each territory contained either one or two, depending on whether the locus had been replicated). The centroid coordinates of the locus signal were calculated. Hybridization signal from the chromosome territory was then segmented interactively on the basis of pixel thresholding without knowledge of the locus signal, and a region of interest was manually defined to include all of the detectable territory. An example of a chromosome territory segmentation mask is shown in Fig. 2 a. The area of the territory was calculated. A segmentation disc was dilated out from the locus signal centroid and then eroded until a pixel with zero intensity from the territory signal was found. This was taken to be the nearest edge of the ter-

ritory to the locus, and the radius of the disc was calculated representing the distance from the center of the locus to the nearest edge of the territory ( $\mu$ m). A similar procedure was used to determine the distance between the territory centroid and territory edge. Because actual territory size varied between different cell types and at different cell cycle stages, we normalized the locus to territory edge distance by dividing it by the radius of a circle of equal area to the territory. A value of 0.0 thus denotes a locus at the edge of a chromosome territory, and 1.0 denotes a locus at the theoretical center of that circle. Negative values indicate loci that appear to be located outside of the visible limits of the chromosome territory. In practice, values of 1.0 are not seen because territories are not circular, and the actual territory centroid had a mean value of  $0.64 \pm 0.02$  along this theoretical radius for HSA11p and  $0.58 \pm 0.03$  for MMU2. To assess the reproducibility of this method of analysis, the same set of 50 images were analyzed independently by two different observers. The actual distance ( $0.53 \pm 0.05$  and  $0.58 \pm 0.04$   $\mu$ m), and the normalized distance ( $0.31 \pm 0.02$  and  $0.32 \pm 0.02$ ) of the PAX6 gene from the HSA11p territory surface in lymphoblasts were similar in both cases.

To analyze 3D images, signals from the chromosome territory and the cosmid or BAC probe were converted to gray scale images. Regions corresponding to the chromosome territory and probe were segmented manually in each plane using the program MAPaint (<http://genex.hgu.mrc.ac.uk/Software/paint/>). Chromosome domains were delineated by thresholding, which segments connected regions within the image that have the same signal intensities. The probe signal was delineated using the "paint ball" facility. The volume of the chromosome territory domain and the minimum distance between the center-of-mass of the probe domain and the surface of the territory were calculated. Spatial coordinates were normalized using the measured voxel size (x 1, y 1, z 5) to compensate for 0.5- $\mu$ m spacing between consecutive image planes.

For visualization of the chromosome and probe domains in context, the nucleus was also segmented using the same "thresholding" facility. The AVS/Express visualization system (Advanced Visual Systems, Inc.) was used to produce a surface-rendered 3D view, and this was used to make an MPEG movie by rotation around the x axis (<http://www.mpeg.org>).

The significance of differences in the relative positions of different loci using 2D and 3D analysis techniques was tested by one-way analysis of variation using MINITAB software (release 12.21). The results of all analyses on WAGR showed that the component of variance between the intra-territory position of probes in different nuclei was not significantly greater than the variance between intraterritory position within homologous chromosomes within a single nucleus. Therefore, the territory was taken as the basic unit of observation.

### RT-PCR

5  $\mu$ g RNA extracted from cells using Bio/RNA-XCell (Bio/Gene) were reverse transcribed at 42°C for 2 h using 20 U M-MuLV reverse transcriptase (BCL) in a volume of 20  $\mu$ l containing 50 mM Tris, pH 8.3, 75 mM KCl, 3 mM MgCl<sub>2</sub>, 10 mM DTT, 20 U RNase inhibitor (BCL), and 200 ng random hexanucleotides (BCL) (+RT). Identical reactions without reverse transcriptase were performed as a control (-RT). The products of both reactions were then amplified with primer pairs to each of the four genes of the human WAGR locus in a total of 25  $\mu$ l for the *PAXNEB* gene and 50  $\mu$ l for the other three genes. For *WT1*, D609 from exon 1 and D610 from exon 6 amplify a 686-bp fragment (Williamson, 1996). For *RCN*, primers G829 and G830 amplify a 795-bp fragment containing most of the coding region (Kent et al., 1997); *PAX6* primers B251 (from exon 7) and C402 (exon13) amplify a 898-bp fragment (Hanson et al., 1993). For *PAXNEB*, primers 023 (5'-CTCTCTTTCAGCCTGCATC) from exon 7 and 041 (5'-TCCCTAGTCAGGTGC) from exon 10 amplify a 396-bp fragment using the following conditions: 94°C for 5 min and then (94°C for 45s, 56°C for 45 s, and 72°C for 45 s)  $\times$  30 (D.A. Kleinjan, personal communication).

We thank Hongen Zhang, Michael Bittner, and Jeffrey Trent (National Institutes of Health, Bethesda, MD) for providing us with HSA11p paint, Dirk-Jan Kleinjan and Colin Miles for mouse BACs, and Irina Solovei (University of Munich, Munich, Germany) for MMU2 paint. The CD5a cell line was a gift from Alan Prescott (University of Dundee, Dundee, UK). We are indebted to Andrew Carothers for input into data analysis and statistics.

N. Mahy was supported by a studentship from the Medical Research Council, and W.A. Bickmore is a Centennial Fellow of the James. S. McDonnell Foundation.

Submitted: 19 November 2001

Revised: 26 March 2001

Accepted: 26 March 2001

## References

- Abranches, R., A.F. Beven, L. Aragon-Alcaide, and P.J. Shaw. 1998. Transcription sites are not correlated with chromosome territories in wheat nuclei. *J. Cell Biol.* 143:5–12.
- Belmont, A.S., S. Dietzel, A.C. Nye, Y.G. Strukov, and T. Tumber. 1999. Large-scale chromatin structure and function. *Curr. Opin. Cell Biol.* 11:307–311.
- Berg-Bakker, C.A., A. Hagemeijer, E.M. Franken-Postma, V.T. Smit, P.J. Kuppen, H.H. Ravenswaay Claasen, C.J. Cornelisse, and P.I. Schrier. 1993. Establishment and characterization of 7 ovarian carcinoma cell lines and one granulosa tumor cell line: growth features and cytogenetics. *Int. J. Cancer.* 53:613–620.
- Bickmore, W.A., and A.D. Carothers. 1995. Factors affecting the timing and imprinting of replication on a mammalian chromosome. *J. Cell Sci.* 108:2801–2809.
- Boyle, S., S. Gilchrist, J.M. Bridger, N.L. Mahy, J.A. Ellis, and W.A. Bickmore. 2001. The spatial organisation of human chromosomes in the nuclei of normal and emerin-mutant cells. *Hum. Mol. Genet.* 10:211–219.
- Clemson, C.M., and J.B. Lawrence. 1996. Multifunctional compartments in the nucleus: insights from DNA and RNA localization. *J. Cell. Biochem.* 62: 181–190.
- Cmarko, D., P.J. Verschure, T.E. Martin, M.E. Dahmus, S. Krause, X.D. Fu, R. van Driel, and S. Fakan. 1999. Ultrastructural analysis of transcription and splicing in the cell nucleus after bromo-UTP microinjection. *Mol. Biol. Cell.* 10:211–223.
- Craig, J.M., and W.A. Bickmore. 1994. The distribution of CpG islands in mammalian chromosomes. *Nat. Genet.* 7:376–382.
- Cremer, T., and C. Cremer. 2001. Chromosome territories, nuclear architecture and gene regulation in mammalian cells. *Nat. Rev. Genet.* 2:292–301.
- Croft, J.A., J.M. Bridger, S. Boyle, P. Perry, P. Teague, and W.A. Bickmore. 1999. Differences in the localization and morphology of chromosomes in the human nucleus. *J. Cell Biol.* 145:1119–1131.
- Dietzel, S., K. Schiebel, G. Little, P. Edelmann, G.A. Rappold, R. Eils, C. Cremer, and T. Cremer. 1999. The 3D positioning of ANT2 and ANT3 genes within female X chromosome territories correlates with gene activity. *Exp. Cell Res.* 252:363–375.
- Eils, R., S. Dietzel, E. Bertin, E. Schrock, M.R. Speicher, T. Ried, M. Robert-Nicoud, C. Cremer, and T. Cremer. 1996. Three-dimensional reconstruction of painted human interphase chromosomes: active and inactive X chromosome territories have similar volumes but differ in shape and surface structure. *J. Cell Biol.* 135:1427–1440.
- Engelkamp, D., P. Rashbass, A. Seawright, and V. van Heyningen. 1999. Role of Pax6 in development of the cerebellar system. *Development.* 126:3585–3596.
- Engemann, S., M. Stroedicke, M. Paulsen, O. Franck, R. Reinhardt, N. Lane, W. Reik, and J. Walter. 2000. Sequence and functional comparison in the Beckwith-Wiedemann region: implications for a novel imprinting centre and extended imprinting. *Hum. Mol. Genet.* 9:2691–2706.
- Fakan, S., and P. Nobis. 1978. Ultrastructural localization of transcription sites and of RNA distribution during the cell cycle of synchronized CHO cells. *Exp. Cell Res.* 113:327–337.
- Fantes, J.A. 1997. Molecular cytogenetics of 11p. Ph.D. thesis. The Open University, Milton Keynes, UK. 184 pp.
- Fantes, J.A., K. Oghene, S. Boyle, S. Danes, J.M. Fletcher, E.A. Bruford, K. Williamson, A. Seawright, A. Schedl, I. Hanson, and V. van Heyningen. 1995. A high-resolution integrated physical, cytogenetic, and genetic map of human chromosome 11: distal p13 to proximal p15.1. *Genomics.* 25:447–461.
- Gawin, B., A. Niederfuhr, N. Schumacher, H. Hummerich, P.F. Little, and M. Gessler. 1999. A 7.5 Mb sequence-ready PAC contig and gene expression map of human chromosome 11p13-p14.1. *Genome Res.* 9:1074–1086.
- Guan, X.Y., H. Zhang, M. Bittner, Y. Jiang, P. Meltzer, and J. Trent. 1996. Chromosome arm painting probes. *Nat. Genet.* 12:10–11.
- Habermann, F.A., M. Cremer, J. Walter, G. Kreth, J. von Hase, K. Bauer, J. Wienberg, C. Cremer, T. Cremer, and I. Solovej. 2001. Arrangements of macro- and microchromosomes in chicken cells. *Chromosome Res.* 9:569–584.
- Hanson, I.M., A. Seawright, K. Hardman, S. Hodgson, D. Zaletayev, G. Fekete, and V. van Heyningen. 1993. PAX6 mutations in aniridia. *Hum. Mol. Genet.* 2:915–920.
- Hastie, N.D. 1994. The genetics of Wilms' tumor—a case of disrupted development. *Annu. Rev. Genet.* 28:523–558.
- Hooper, M., K. Hardy, A. Handyside, S. Hunter, and M. Monk. 1987. HPRT-deficient (Lesch-Nyhan) mouse embryos derived from germline colonization by cultured cells. *Nature.* 326:292–295.
- Jentsch, I., I.D. Adler, N.P. Carter, and M.R. Speicher. 2001. Karyotyping mouse chromosomes by multiplex-FISH (M-FISH). *Chromosome Res.* 9:211–214.
- Jenuwein, T., and C.D. Allis. 2001. Translating the histone code. *Science.* 293: 1074–1080.
- Kent, J., M. Lee, A. Schedl, S. Boyle, J. Fantes, M. Powell, N. Rushmere, C. Abbott, V. van Heyningen, and W.A. Bickmore. 1997. The reticulocalbin gene maps to the WAGR region in human and to the Small eye Harwell deletion in mouse. *Genomics.* 42:260–267.
- Kleinjan, D.A., A. Seawright, G. Elgar, and V. van Heyningen. 2002. Characterisation of a novel gene adjacent to PAX6, revealing synteny conservation with functional significance. *Mamm. Genome.* 13:102–107.
- Kurz, A., S. Lampel, J.E. Nickolenko, J. Bradl, A. Benner, R.M. Zirbel, T. Cremer, and P. Lichter. 1996. Active and inactive genes localize preferentially in the periphery of chromosome territories. *J. Cell Biol.* 135:1195–1205.
- Mahy, N.L., W.A. Bickmore, T. Tumber, and A.S. Belmont. 2000. Linking large-scale chromatin structure with nuclear function. In *Chromatin Structure and Gene Expression*. S.C.R. Elgin and J.L. Workman, editors. Oxford University Press, Oxford, UK. 300–321.
- Miles, C., G. Elgar, E. Coles, D.J. Kleinjan, V. van Heyningen, and N. Hastie. 1998. Complete sequencing of the Fugu WAGR region from WT1 to PAX6: dramatic compaction and conservation of synteny with human chromosome 11p13. *Proc. Natl. Acad. Sci. USA.* 95:13068–13072.
- Nogami, M., A. Kohda, H. Taguchi, M. Nakao, T. Ikemura, and K. Okumura. 2000. Relative locations of the centromere and imprinted SNRPN gene within chromosome 15 territories during the cell cycle in HL60 cell. *J. Cell Sci.* 113:2157–2165.
- Phair, R.D., and T. Misteli. 2000. High mobility of proteins in the mammalian cell nucleus. *Nature.* 404:604–609.
- Tajbakhsh, J., H. Luz, H. Bornfleth, S. Lampel, C. Cremer, and P. Lichter. 2000. Spatial distribution of GC- and AT-rich DNA sequences within human chromosome territories. *Exp. Cell Res.* 255:229–237.
- Tanabe, H., S. Müller, M. Neusser, J. von Hase, E. Calcagno, M. Cremer, I. Solovej, C. Cremer, and T. Cremer. 2002. Evolutionary conservation of chromosome territory arrangements in cell nuclei from higher primates. *Proc. Natl. Acad. Sci. USA.* 99:4424–4429.
- Tumber, T., G. Sudlow, and A.S. Belmont. 1999. Large-scale chromatin unfolding and remodeling induced by VP16 acidic activation domain. *J. Cell Biol.* 145: 1341–1354.
- Verschure, P.J., I. van Der Kraan, E.M. Manders, and R. van Driel. 1999. Spatial relationship between transcription sites and chromosome territories. *J. Cell Biol.* 147:13–24.
- Visser, A.E., R. Eils, A. Jauch, G. Little, P.J. Bakker, T. Cremer, and J.A. Aten. 1998. Spatial distributions of early and late replicating chromatin in interphase chromosome territories. *Exp. Cell Res.* 243:398–407.
- Volpi, E.V., E. Chevret, T. Jones, R. Vatcheva, J. Williamson, S. Beck, R.D. Campbell, M. Goldsworthy, S.H. Powis, J. Ragoussis, et al. 2000. Large-scale chromatin organisation of the major histocompatibility complex and other regions of human chromosome 6 and its response to interferon in interphase nuclei. *J. Cell Sci.* 113:1565–1576.
- Wansink, D.G., O.C. Sibon, F.F. Cremers, R. van Driel, and L. de Jong. 1996. Ultrastructural localization of active genes in nuclei of A431 cells. *J. Cell. Biochem.* 62:10–18.
- Weier, H.U., H.D. Kleine, and J.W. Gray. 1991. Labeling of the centromeric region on human chromosome 8 by in situ hybridisation. *Hum. Genet.* 87: 489–494.
- Williams, R.R.E., S. Broad, D. Sheer, and J. Ragoussis. 2002. Subchromosomal positioning of the epidermal differentiation complex (EDC) in keratinocyte and lymphoblast interphase nuclei. *Exp. Cell Res.* 272:163–175.
- Williamson, K.A. 1996. Involvement of the WT1 and PAX6 genes in Wilms' tumour and human malignant mesothelioma. Ph.D. Thesis. University of Edinburgh, Edinburgh, UK. 204 pp.
- Xu, P.X., X. Zhang, S. Heaney, A. Yoon, A.M. Michelson, and R.L. Maas. 1999. Regulation of Pax6 expression is conserved between mice and flies. *Development.* 126:383–395.
- Yokota, H., M.J. Singer, G.J. van den Engh, and B.J. Trask. 1997. Regional differences in the compaction of chromatin in human G0/G1 interphase nuclei. *Chromosome Res.* 5:157–166.
- Zirbel, R.M., U.R. Mathieu, A. Kurz, T. Cremer, and P. Lichter. 1993. Evidence for a nuclear compartment of transcription and splicing located at chromosome domain boundaries. *Chromosome Res.* 1:93–106.